Published in "Nature Climate Change 8 (1): 48–52, 2018"
which should be cited to refer to this work.

Changes in Greenland's peripheral glaciers linked to the North Atlantic Oscillation

A. A. Bjørk[1,2,3*], S. Aagaard[1], A. Lütt[1], S. A. Khan[4], J. E. Box[5], K. K. Kjeldsen[1,4,6], N. K. Larsen[1,7], N. J. Korsgaard[8], J. Cappelen[9], W. T. Colgan[5,10], H. Machguth[11,12], C. S. Andresen[5], Y. Peings[2] and K. H. Kjær[1]

Glaciers and ice caps peripheral to the main Greenland Ice Sheet contribute markedly to sea-level rise[1–3]. Their changes and variability, however, have been difficult to quantify on multi-decadal timescales due to an absence of long-term data[4]. Here, using historical aerial surveys, expedition photographs, spy satellite imagery and new remote-sensing products, we map glacier length fluctuations of approximately 350 peripheral glaciers and ice caps in East and West Greenland since 1890. Peripheral glaciers are found to have recently undergone a widespread and significant retreat at rates of 12.2 m per year and 16.6 m per year in East and West Greenland, respectively; these changes are exceeded in severity only by the early twentieth century post-Little-Ice-Age retreat. Regional changes in ice volume, as reflected by glacier length, are further shown to be related to changes in precipitation associated with the North Atlantic Oscillation (NAO), with a distinct east–west asymmetry; positive phases of the NAO increase accumulation, and thereby glacier growth, in the eastern periphery, whereas opposite effects are observed in the western periphery. Thus, with projected trends towards positive NAO in the future[5,6], eastern peripheral glaciers may remain relatively stable, while western peripheral glaciers will continue to diminish.

Despite comprising less than 5% of the area of the Greenland Ice Sheet (GrIS), peripheral glaciers and ice caps (PGICs) are important contributors to recent sea-level rise, accounting disproportionally for up to 20% of early twenty-first century (2003–2008) Greenland ice loss and sea-level rise[1–3] (see Supplementary Information). As PGICs are predominately land terminating and thus insensitive to marine processes, they provide a more direct measure of glacier sensitivity to atmospheric climate variability. Furthermore, their relatively short glacier reservoir times[7,8], meaning faster mass turnover via enhanced snow and melt fluxes, makes the PGICs react more rapidly to climate variability. We explore the length fluctuations of nearly 350 Greenlandic glaciers that occurred between the ending of the Little Ice Age (LIA) (1890–1910) and 2015 in East and West Greenland (Figs. 1 and 2). The GrIS has behaved differently in those areas, as the western region has lost considerable mass in recent decades, whereas the eastern region has remained stable or even slightly grown since 2000[9,10] (Fig. 1). The sparse glacier extent records available generally document glacier retreat related to rising temperatures[4,11]. However, these records are generally limited to southern and southwestern Greenland. We target two understudied regions with appreciable ice masses peripheral to the ice sheet; the eastern region between 70.5 and 75.0 °N and the western region between 71.0–72.5 °N (see Supplementary Information). By targeting the peripheral glaciers in these two regions, we are able to map the regional glacial response to changes in atmospheric influence during periods with variation in external forcing and intense Arctic climate change.

We use historical photographs from the 1930s, collected by Danish and Norwegian aerial surveys, and in East Greenland also by land-based expeditions by American explorer L. A. Boyd (see Supplementary Information). The historical photos are combined with modern and historical aerial- and satellite imagery that extend the history of the glaciers to the present (Methods and Supplementary Information). Although there are no large-scale photographic datasets available from the onset of the LIA deglaciation, we map the glacial extent from that time based on geomorphological evidence[12] to further expand our glacial observations (see Methods and Supplementary Information). Precise constraints on the regional timing of the LIA deglaciation are, however, sparse. We assign AD 1910 to the onset of the regional LIA deglaciation in East Greenland, and 1890 in West Greenland (see Supplementary Information). The use of high-resolution aerial imagery allows us to produce a detailed LIA-deglaciation map for both regions and thus provide a large-scale, systematic assessment of early glacier change. Detailed evidence of LIA positions, preserved in the landscape as moraines and trimlines[12], makes the study sites well-suited for photogrammetric mapping. The early twentieth century images from the East Greenland expeditions capture the regional response to the end of the LIA; however, no such early regional aerial imagery is available for West Greenland. As a result, a long initial period from the end of the LIA to the first observations in the 1950s slightly smooths the actual magnitude of maximum post-LIA retreat in the West Greenland study area. The large differences in glacier geometry in the studied regions also results in different response times to past climatic changes[13] and frontal change rate responses to climatic changes are thus temporally delayed and smoothed. We avoid surging glaciers in the study by excluding all glaciers that exhibit one

[1]Centre for GeoGenetics, Natural History Museum of Denmark, University of Copenhagen, Copenhagen, Denmark. [2]Earth System Science, University of California, Irvine, CA, USA. [3]NASA Jet Propulsion Lab, Pasadena, CA, USA. [4]DTU Space, National Space Institute, Department of Geodesy, Technical University of Denmark, Kongens Lyngby, Denmark. [5]Geological Survey of Denmark and Greenland (GEUS), Copenhagen, Denmark. [6]Department of Earth Sciences, University of Ottawa, Ottawa, Ontario, Canada. [7]Department of Geoscience, Aarhus University, Aarhus, Denmark. [8]Nordic Volcanological Center, Institute of Earth Sciences, University of Iceland, Reykjavík, Iceland. [9]Danish Meteorological Institute (DMI), Copenhagen, Denmark. [10]Department of Earth and Space Science & Engineering, York University, Toronto, ON, Canada. [11]Department of Geography, University of Zurich (UZH), Zurich, Switzerland. [12]Department of Geosciences, University of Fribourg, Fribourg, Switzerland. *e-mail: andersb@snm.ku.dk

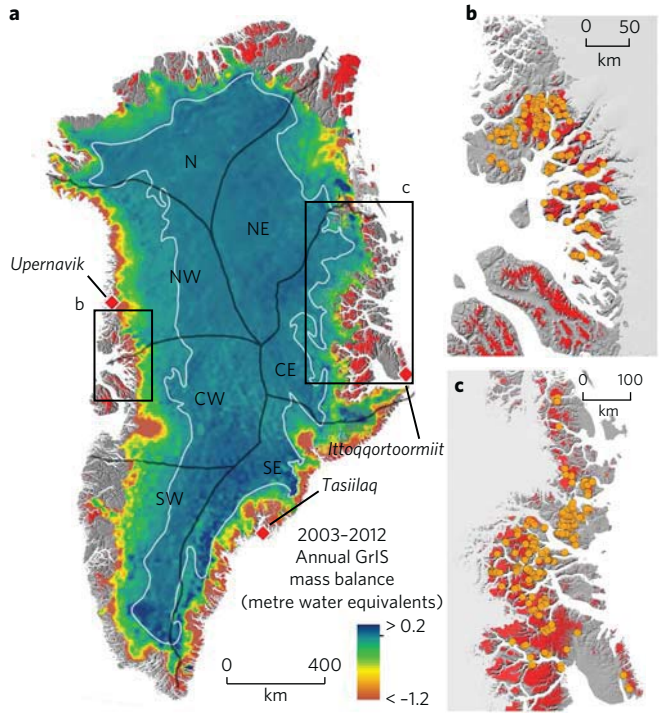

Fig. 1 | PGICs in Greenland and current GrIS mass loss. a, Annual mass balance of the GrIS from 2003 to 2012[9]. The grey line indicates a smoothed 0 m yr^{-1} contour representing the contemporary equilibrium line altitude. Around the ice sheet, peripheral glaciers and ice caps are shown in red polygons. **b**,**c**, Insets show the west and east regions, respectively, with the investigated glaciers highlighted as orange dots.

or more surge features (Methods). Within the East and West study areas, more than 1,000 glaciers could be identified, of which 195 (representing 22% of the region's total glaciated area) were successfully mapped in multiple epochs in East Greenland, and 139 in West Greenland (representing 35 % of the peripheral ice area). This compilation more than quadruples the number of Greenlandic glaciers with a twentieth century length record[14] from 77 to 411 (Methods and Supplementary Information).

We divide the observational period from the LIA deglaciation to present into periods and calculate a rate of glacier length change (m yr^{-1}) for each period (Fig. 2 and Supplementary Information). As these two regions have seen a different climatic development in the past century, we further assess the influence of precipitation variability[15] on the glaciers and investigate an apparent connection to large-scale atmospheric circulation patterns associated with the winter mode of the North Atlantic Oscillation (NAO)[16]. We establish a link between glacier geometry and the NAO-forced precipitation variability in East and West Greenland and subsequently investigate the spatial fingerprint of the NAO on the mass balance of the entire GrIS.

When East Greenland entered the LIA deglaciation, most of its PGICs retreated at an average rate of 22.1 ± 6.4 m yr^{-1} from 1910 to 1932 (Figs. 1 and 2a), almost twice the retreat rate of the 2000–2013 period (12.2 ± 1.8 m yr^{-1}) (Fig. 2). The rapid retreat during and after the warming of the 1920s in East Greenland can be partly explained by the glacier fronts being situated in lower elevations than at present[4], and with an initial LIA retreat occurring on flat terrain (see Supplementary Information). However, the near doubling of retreat rates compared with the present is surprising, given that local temperatures at the nearest long-term meteorological station in southeast Greenland were in the 2010s approximately 1 °C warmer than during the peak early twentieth century warming (Fig. 2). This suggests that the extent of the PGICs was more out of balance with the climate that followed the LIA than at present. A similar rapid early twentieth century retreat had also been documented in Sourtheast[4] and Southwest Greenland[11]. Because of missing early twentieth century images from the western region, it cannot be excluded that a similar change took place there. Interestingly, many of the eastern glaciers in the record presented here also shift from retreat to advance in the mid-1960s, when East Greenland temperatures were dropping about 1 °C in a decade (Fig. 2). From 1966–1973, nearly half of the eastern glaciers were advancing, yielding an average retreat rate for the region of -3.9 ± 4.8 m yr^{-1}. This suggests that the glaciers are indeed responding rapidly to changes in atmospheric climate forcing at a decadal timescale[17], and with a decline in precipitation, this widespread advance was governed by the regional cooling. The brief 1966–1973 advance in East Greenland, however, was followed by a period of widespread retreat (on average 7.7 ± 2.2 m yr^{-1}) during 1973–1987, as temperatures rose again by around 1.5 °C. Although average temperatures were around 1.5 °C warmer in the 1980s and 1990s compared with the previous decades, the retreat rates remained constant (6.7 ± 1.3 m yr^{-1}) from 1987 to 2000. Available records of melt-day anomalies (Supplementary Information), which suggest a clear increase in the number of melt days from 1979 to 2012, show no correlation with glacier length records. We suggest that this steady rate during warming was partly a result of changes in snow accumulation rates, which, in contrast to the west coast, peaked for this region during the 1990s (Fig. 2). In contrast to the east coast, the western peripheral glaciers presented here are undergoing a constant and marked retreat during the same period, culminating with a substantial increase in retreat rate (+85%) during the most recent observational period.

While a conventional explanation for accumulation variability is sea-ice-modulated moisture availability[18], we find no direct link between available precipitation records and existing sea-ice concentration datasets (Supplementary Information). Likewise, the sharp accumulation increase does not coincide with big changes in sea-ice transport through the Fram Straight[19]. There is, however, a clear link between the accumulation record and periods with strong modes of atmospheric circulation[20–23], which are represented in this study by the winter mode of the NAO (Fig. 2 and Supplementary Information). The connection between East Greenland precipitation and NAO is positive, meaning that there is more precipitation during NAO+. Both spatial and temporal differences between Greenland precipitation variability and large-scale atmospheric circulation are represented by the NAO and other indexes[23,24]. We explore the apparent spatial partitioning of Greenland precipitation changes, which is divided north to south along the central ice sheet. This division is reflected by increased precipitation in West Greenland and decreased precipitation in East Greenland during NAO− and vice versa during NAO+.

We compare the spatial precipitation patterns for the two most pronounced phases of strong winter NAO recorded during the twentieth century (Table 1 and Fig. 3). These periods of strong winter NAO− (1962–1971) and NAO+ (1988–1995) indicate that the connection between NAO and regional precipitation is strongest in East Greenland and is opposite during strong NAO+ and NAO− phases (Fig. 2), whereas NAO influence on precipitation is not apparent during relatively neutral NAO periods. During NAO− (Fig. 3a), the weakening of its two atmospheric centres of action (Azores High and Icelandic Low) results in decreased westerlies and storm track activity over the North Atlantic. NAO− is associated with warmer temperatures over Greenland, especially in the west. By contrast, NAO+ is associated with reinforced westerlies, storm track activity and colder temperatures over Greenland. The accumulation rate anomalies for strong NAO− and NAO+ phases (Fig. 3) are considerable when integrated over all East Greenland

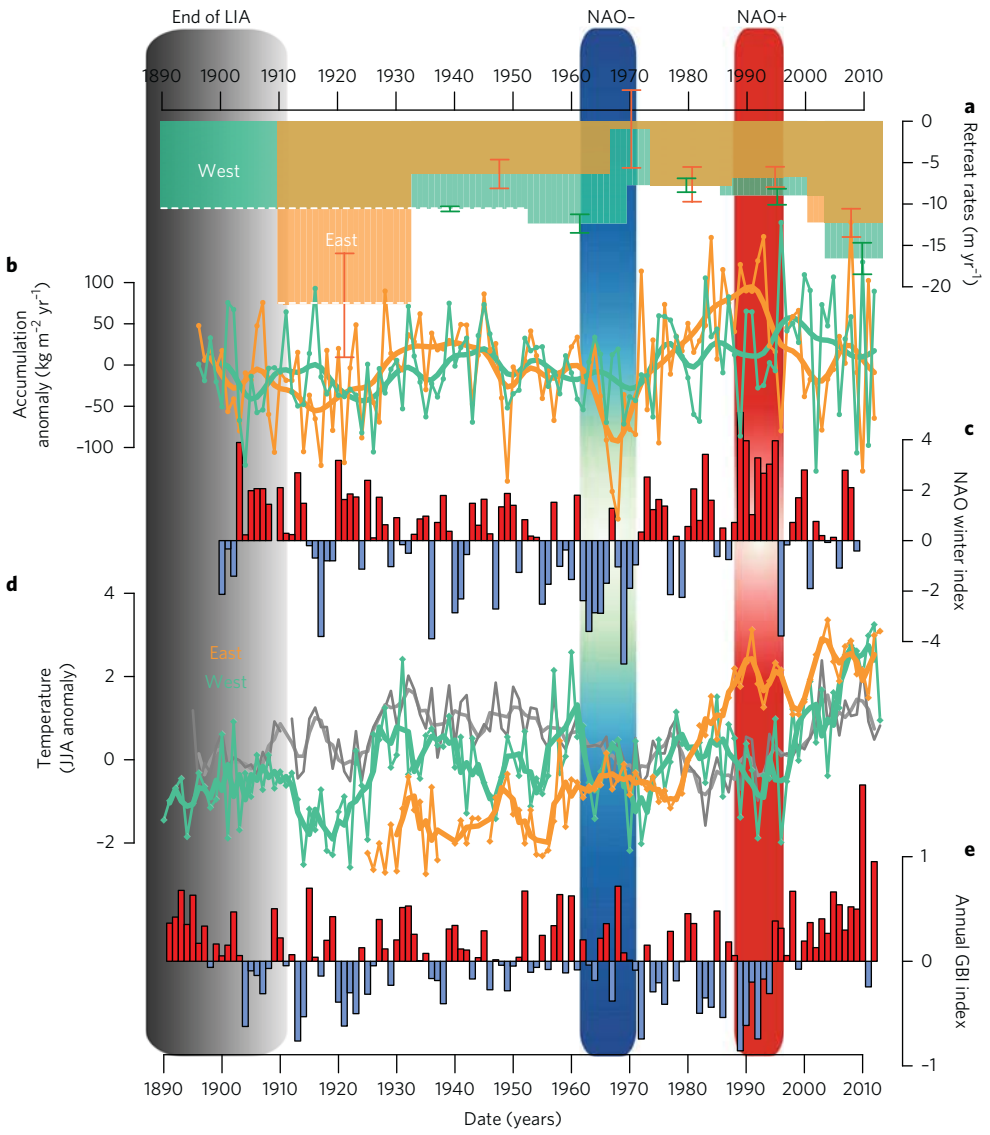

Fig. 2 | Comparison of glacier retreat with changes in climate and atmospheric circulation. a, Retreat rates (m yr^{-1}) for glacier clusters in East (orange) and West (green) Greenland divided into observational periods. Error bars represent digitizing and rectification uncertainties. Timing of the onset of the first observations is uncertain. **b**, Reconstructed accumulation averaged for the two study regions[12,15], with east shown in orange and west in green. **c**, Station-based winter NAO index[16]. **d**, Temperature measurements from meteorological stations[32], and an additional station (grey line) from southeast Greenland. **e**, Annual Greenland blocking index[21]. For accumulation and temperature, thin lines represent annual values and bold lines are Gaussian smoothed values. For NAO and GBI, red bars represent positive indices and blue bars indicate negative indices.

regions of the ice sheet (Fig. 3b and Table 1, see also Supplementary Information). During the NAO− period of 1962–1971, this was equivalent to a 9.0 ± 0.7 Gt yr^{-1} (−17.4%) deficit in annual accumulation in the region (percentages refer to twentieth century mean accumulation; see Methods). Conversely, during the NAO+ period of 1988–1995, the region received an extra 5.3 ± 0.4 Gt yr^{-1} (7.6%) of annual accumulation. NAO-related accumulation variability in West Greenland is opposite to, and more subdued than, the accumulation variability in East Greenland. West Greenland received +4.3% and −3.0% in annual accumulation during NAO− and NAO+, respectively. These differences indicate that the accumulation rates of PGICs in East Greenland are up to four times more sensitive to NAO changes than those in West Greenland. Integrated over the entire ice sheet, east–west compensation slightly masks the NAO precipitation effect, resulting in anomalies of −7.9% during the NAO− period and +1.3% during the NAO+ period. As accumulation variability does not oscillate at the ice divide but oscillates closer to the western ice margin, western ice sheet regions receive a mixed signal (Fig. 3), which is also reflected in the lower anomalies (Table 1). As with existing studies[20,23,24], we find that the NAO signal is important at the regional scale, but spatially compensating variability minimizes its influence on the ice sheet as a whole. As NAO-driven accumulation changes increase towards the coasts, accumulation rate changes exceeding −20% and +25% have significant consequences for the geometry of PGICs and regional ice sheet topography. Averaged over the entire region, including ice-free terrain, the accumulation anomalies over peripheral glaciers are similar, but with slightly higher anomalies (Table 1), indicating a higher coastal–NAO correlation (Fig. 3).

We demonstrate an inter-decadal regional response of a large sample of peripheral glaciers in East and West Greenland to climate variability over more than a century. The precipitation in the eastern and western sections of Greenland are partly in an anti-phase with the variability driven by large-scale circulation patterns, which are

Table 1 | Accumulation rate anomalies for GrIS regions

Region	NAO− (1962–1971)			NAO+ (1988–1995)		
	Total	Anomaly	Anomaly	Total	Anomaly	Anomaly
	Gt yr^{-1}	Gt yr^{-1}	(%)	Gt yr^{-1}	Gt yr^{-1}	(%)
Central-east GrIS	42.6 ± 3.4	−9.0 ± 0.7	−17.4	56.9 ± 4.5	5.3 ± 0.4	10.2
Northeast GrIS	30.4 ± 2.4	−3.0 ± 0.2	−8.9	34.6 ± 2.8	1.2 ± 0.1	3.7
North GrIS	38.1 ± 3.0	1.6 ± 0.1	4.3	40.0 ± 6.2	3.4 ± 0.3	9.3
Northwest GrIS	110.2 ± 8.8	4.2 ± 0.3	4.0	102.8 ± 8.2	−3.2 ± 0.3	−3.0
Central-west GrIS	98.0 ± 7.8	−2.9 ± 0.2	−2.9	101.0 ± 8.1	0.1 ± 0.01	0.1
Southwest GrIS	138.3 ± 11.1	−3.9 ± 0.3	−2.7	143.0 ± 11.4	0.8 ± 0.1	0.6
Southeast GrIS	248.3 ± 19.9	−47.4 ± 3.8	−16.0	298.5 ± 23.9	2.8 ± 0.2	1.0
Entire GrIS	706.1 ± 56.5	−60.3 ± 4.8	−7.9	776.9 ± 62.2	10.5 ± 0.8	1.4
PGICs East			−22.4			25.3
PGICs West			3.8			−7.9

Accumulation rate anomalies for the two periods of NAO− and NAO+ are shown for the entire ice sheet and for seven ice sheet regions. The regional subdivision can be seen in Fig. 1. For the peripheral regions, the accumulation is averaged for the entire region, including the ice-free terrain as SMB model spatial resolution does not allow division of small glaciers—therefore no absolute values are given for these regions. Reference period is 1900–1999.

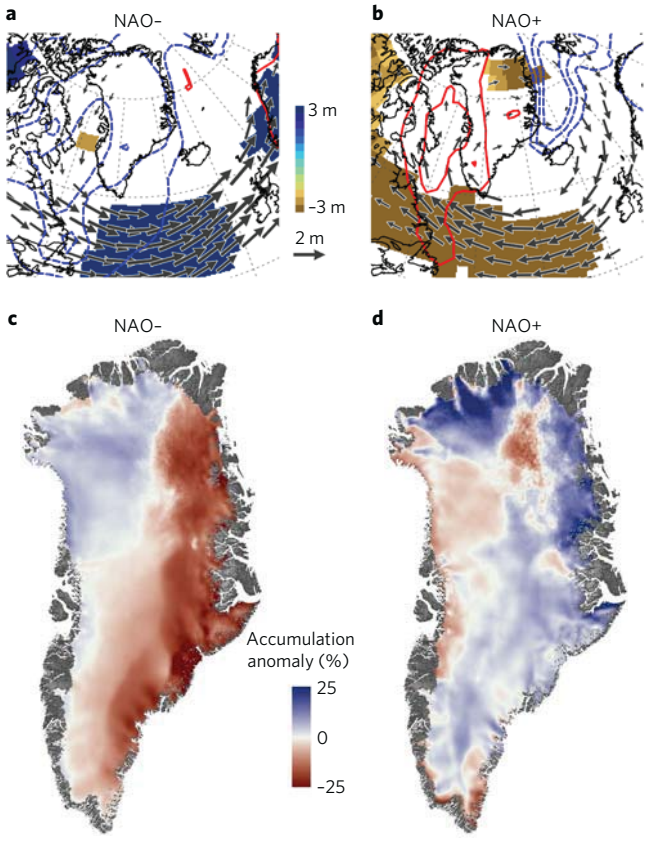

Fig. 3 | NAO circulation patterns and associated accumulation anomalies. **a**,**b**, Anomalies in the transient eddy activity (shading, in m), 850 hPa wind (vectors in m s^{-1}), and 2 m temperature (red/blue contours, in °C)[31], with winter anomalies estimated relative to the 1948–2016 climatology. Only anomalies that are significant at the 95% confidence level are shown for the transient eddy activity and the 850 hPa wind. **c**,**d**, GrIS annual accumulation anomalies[12,15] for two distinct periods of NAO− (1962–1971) and NAO+ (1988–1995). Anomalies are calculated from a 1900–1999 normal period (see also Methods and Supplementary Information).

represented by the winter mode of the NAO. This precipitation anomaly can greatly affect the mass balance of Greenland's PGICs and therefore also the glacier lengths. As the PGICs of Greenland are already contributing significantly to global sea-level rise, and will probably contribute between 20 ± 8 mm (under future climate scenario RCP4.5) and 30 ± 8 mm (under future climate scenario RCP8.5) between 2006 and 2100[25,26], their future remains extremely important despite their relatively small size (RCP; representative concentration pathway). Our results show that the PGICs of Greenland have gone into widespread and rapid retreat, only exceeded in severity by the LIA deglaciation when baseline conditions were substantially different from the present. Furthermore, our findings suggest that the east–west accumulation asymmetry of a prolonged NAO phase would have a substantial influence on glacier and ice sheet geometry, with the east coast region being up to four times more sensitive to these changes. For the ice sheet as a whole, if the NAO is to remain in a predominantly positive phase (similar to the 1985–1995 anomaly) throughout the twenty-first century as has been suggested[5,6], the consequence may well be a continuous stable east coast and a diminishing west coast, resulting in a positive surface mass balance (SMB) anomaly of around 10 Gt yr^{-1}. This is a substantial amount equaling around 16% of the annual mass loss of the ice sheet from 1900 to 2010[12]. Our results therefore stress the need to specifically account for future NAO variability in Greenland SMB models, both for short- and long-term modelling of the cryosphere in the North Atlantic realm, as well as for evaluating the regional signal in past SMB reference periods[27,28]. Moreover, it also seems essential to address the large-scale atmospheric variability when interpreting regional changes in the ice volume of both the GrIS and PGICs.

Methods

Methods, including statements of data availability and any associated accession codes and references, are available at https://doi.org/10.1038/s41558-017-0029-1.

Received: 3 April 2017; Accepted: 15 November 2017;
Published online: 18 December 2017

References

1. Bolch, T. et al. Mass loss of Greenland's glaciers and ice caps 2003–2008 revealed from ICESat laser altimetry data. *Geophys. Res. Lett.* **40**, 875–881 (2013).
2. Colgan, W. et al. Hybrid glacier inventory, gravimetry and altimetry (HIGA) mass balance product for Greenland and the Canadian Arctic. *Remote Sens. Environ.* **168**, 24–39 (2015).
3. Gardner, A. et al. A reconciled estimate of glacier contributions to sea level rise: 2003 to 2009. *Science* **340**, 852–857 (2013).

4. Bjørk, A. A. et al. An aerial view of 80 years of climate-related glacier fluctuations in southeast Greenland. *Nat. Geosci.* **5**, 427–432 (2012).
5. IPCC *Climate Change 2013: The Physical Science Basis* (eds Stocker, T. F. et al.) (Cambridge Univ. Press, Cambridge, 2013).
6. Gillett, N. P. & Fyfe, J. C. Annular mode changes in the CMIP5 simulations. *Geophys. Res. Lett.* **40**, 1189–1193 (2013).
7. Machguth, H. et al. The future sea-level rise contribution of Greenland's glaciers and ice caps. *Environ. Res. Lett.* **8**, 025005 (2013).
8. Bintanja, R. & Selten, F. M. Future increases in Arctic precipitation linked to local evaporation and sea-ice retreat. *Nature* **509**, 479–482 (2014).
9. Khan, S. A. et al. Sustained mass loss of the northeast Greenland ice sheet triggered by regional warming. *Nat. Clim. Change* **4**, 292–299 (2014).
10. Csatho, B. M. et al. Laser altimetry reveals complex pattern of Greenland Ice Sheet dynamics. *Proc. Natl Acad. Sci. USA* **111**, 18478–18483 (2014).
11. Leclercq, P. W. et al. Brief communication "Historical glacier length changes in West Greenland". *Cryosphere* **6**, 1339–1343 (2012).
12. Kjeldsen, K. K. et al. Spatial and temporal distribution of mass loss from the Greenland Ice Sheet since AD 1900. *Nature* **528**, 396–400 (2015).
13. Bahr, D. B., Pfeifer, W. T., Sassolas, C. & Meier, M. F. Response time of glaciers as a function of size and mass balance: 1. Theory. *J. Geophys. Res.* **103**, 9777–9782 (1998).
14. Leclercq, P. W. et al. A data set of worldwide glacier length fluctuations. *Cryosphere* **8**, 659–672 (2014).
15. Box, J. E. Greenland ice sheet mass balance reconstruction. Part II: Surface mass balance (1840–2010). *J. Clim.* **26**, 6974–6989 (2013).
16. Hurrell, J. W. Decadal trends in the North Atlantic Oscillation: regional temperatures and precipitation. *Science* **269**, 676–679 (1995).
17. Johannesson, T., Raymond, C. & Waddington, E. Time-scale for adjustment of glaciers to changes in mass balance. *J. Glaciol.* **35**, 355–369 (1989).
18. Hebbeln, D., Dokken, T., Andersen, E. S., Hald, M. & Elverhøi, A. Moisture supply for northern ice-sheet growth during the Last Glacial Maximum. *Nature* **370**, 357–360 (1994).
19. Schmith, T. & Hansen, C. Fram Strait ice export during the nineteenth and twentieth centuries reconstructed from a multiyear sea ice index from southwestern Greenland. *J. Clim.* **16**, 2782–2791 (2003).
20. Hanna, E. et al. Greenland Ice Sheet surface mass balance 1870 to 2010 based on twentieth century reanalysis, and links with global climate forcing. *J. Geophys. Res.* **116**, D24121 (2011).
21. Hanna, E., Cropper, T. E., Hall, R. J. & Cappelen, J. Greenland blocking index 1851–2015: a regional climate change signal. *Int. J. Climatol.* **36**, 4847–4861 (2016).
22. Auger, J. D., Birkel, S. D., Maasch, K. A., Mayewski, P. A. & Schuenemann, K. C. Examination of precipitation variability in southern Greenland. *J. Geophys. Res. Atmos.* **122**, 6202–6216 (2017).
23. Appenzeller, C., Schwander, J., Sommer, S. & Stocker, T. F. The North Atlantic Oscillation and its imprint on precipitation and ice accumulation in Greenland. *Geophys. Res. Lett.* **25**, 1939–1942 (1998).
24. Burgess, E. W. et al. A spatially calibrated model of annual accumulation rate on the Greenland Ice Sheet (1958–2007). *J. Geophys. Res.* **115**, F02004 (2010).
25. Marzeion, B., Jarosch, A. H. & Hofer, M. Past and future sea-level change from the surface mass balance of glaciers. *Cryosphere* **6**, 1295–1322 (2012).
26. Radić, V. et al. Regional and global projections of twenty-first century glacier mass changes in response to climate scenarios from global climate models. *Clim. Dyn.* **42**, 37–58 (2014).
27. van den Broeke, M. et al. Partitioning recent Greenland mass loss. *Science* **326**, 984–986 (2009).
28. Rignot, E., Box, J. E., Burgess, E. & Hanna, E. Mass balance of the Greenland ice sheet from 1958 to 2007. *Geophys. Res. Lett.* **35**, L20502 (2008).
31. Kalnay, E. et al. The NCEP/NCAR 40-year reanalysis project. *Bull. Am. Meteorol. Soc.* **77**, 437–471 (1996).
32. Cappelen, J. *Greenland—DMI Historical Climate Data Collection 1784-2016* DMI Report 17-04 (Danish Meteorological Institute, 2017).

Acknowledgements

A.A.B. was supported by the Independent Research Fund Denmark (grant DFF-610800469) and VILLUM Foundation (grant 10100), and by the Inge Lehmann Scholarship from the Royal Danish Academy of Science and Letters. K.K.K was supported by Independent Research Fund Denmark (grant DFF-4090-00151).C.S.A. and N.K.L. acknowledge support from the VILLUM Foundation (grant no. 10100 and grant no. VRK023440). We are also grateful for the support from the former National Danish Survey and Cadastre, now Department of Data-supply and Efficiency, and the Norwegian Polar Institute without whose help this study could not have been realized.

Author contributions

A.A.B. and K.H.K. designed the study. S.A., A.L. and A.A.B. performed the analysis of aerial photographs and satellite imagery. J.E.B., W.T.C. and K.K.K. created and analysed accumulation and temperature records. S.A.K., C.S.A., N.K.L., N.J.K., H.M., J.C. and Y.P. supplied the data for analysis in the discussion. All authors contributed to the discussion of the results and the writing of the manuscript.

Competing interests

The authors declare no competing financial interests.

Additional information

Supplementary information is available for this paper at https://doi.org/10.1038/s41558-017-0029-1.

Reprints and permissions information is available at www.nature.com/reprints.

Correspondence and requests for materials should be addressed to A.A.B.

Publisher's note: Springer Nature remains neutral with regard to jurisdictional claims in published maps and institutional affiliations.

Methods

All historical images were scanned at high resolution (>600 dpi) and subsequently georeferenced to a 1985–1987 ortho-photograph in 2 m resolution. Rectification and selection of acceptable images was done following ref. [4]. Newer images include Corona (1965, 1966 and 1967), Landsat (1973, 2000 and 2013) satellite imagery and ortho-rectified aerial photographs used for geo-rectification (1985–1987)[29]. Glacier lengths recorded in 1985 images have been normalized to 1987. All retreat rates from the early 1930s are normalized to 1932. We map the maximum position of the LIA glacial extent by digitizing end moraines and trimlines in the 1980s 2 m ortho-rectified aerial image[29], which also serves as a basis for all rectifications of other imagery.

Glacier length measurements follow the procedures described previously[4]. Because some glacier tongues are very narrow, a single point has been placed at the outer margin instead of measuring length changes over the entire width of the frontal lobe. In these instances, this resulted in a more precise length measurement, as the narrow glacier tongues tend to retreat with a uniform geometry. In these cases, length changes have been calculated at the outermost point along the centre flow line. A number of glaciers have been discarded from the dataset because the glaciers were surge-type glaciers or located within known surge clusters. We performed a vigorous surge identification, excluding glaciers with looped moraines, glaciers with crevasse squeeze ridges in the fore field, glaciers advancing more than 50 m yr^{-1} and glaciers with a collapsed accumulation zone.

Digitizing accuracies are calculated as the combination of pixel size and the error from the ortho-photo used for geo-rectification following the procedure described previously[4]. Retreat rate uncertainties are calculated as the root of the sum of squares of the digitizing and rectification uncertainty of the two observations used for each period (see also Supplementary Information). An additional uncertainty has been added to the 1910–1932 retreat rates for East Greenland to account for uncertainty in the timing of the LIA deglaciation, specifically ±5 years, which results in additional uncertainty for the 1910–1932 rate of ±3.6 m yr^{-1}. This is included in the overall uncertainty for the 1910–1932 period of ±6.4 m yr^{-1}. Similarly, we have included ±5 years to the LIA deglaciation timing in West Greenland, which increases the uncertainty of the first observational period by 18%.

The normal period for calculation of NAO anomalies was set to 1900–1999, as this period encompasses the most recent phases of distinct NAO+ and NAO− phases. Precipitation records[15] were calibrated to increase agreement to RACMO2.1/GR[12,30] for the period 1960–1999, whereas, owing to a sharp decrease in accumulation records from ice cores, precipitation fields from RACMO2.1/GR for 2000–2012 were incorporated, ultimately yielding an uncertainty of 8.0%[12]. For accumulation anomalies, results with alternative normal periods were also tested (Supplementary Table 3 and Supplementary Information). Temperature changes in Fig. 2 are derived from coastal meteorological stations (ref. [32]) and locations shown in Fig. 1.

The Greenland Ice Sheet is subdivided regionally[12]. Average accumulation values for the entire PGIC region studied were used, to account for the coarse model resolution, which does not justify studies on individual glacier level. As a result of the coarse resolution of the SMB model, we are only providing absolute accumulation anomalies for the Greenland Ice Sheet and not for the PGICs.

Climate reanalysis (NCEP–NCAR)[31] is used to assess atmospheric circulation, or transient eddy, anomalies in 850 hPa wind, sea-level pressure, and 2 m temperature, relative to 1948–2016 climatology. Only anomalies that are significant at the 95% confidence level are shown for the transient eddy activity and the 850 hPa wind. The transient eddy activity in storm track is derived from the monthly standard deviation of the 2–6-day band pass-filtered daily Z500 (here expressed in m).

Data availability. The data that support the findings of this study are available in the Supplementary Information accompanying this paper and from the corresponding author upon request.

References

29. Korsgaard, N. J. et al. Digital elevation model and orthophotographs of Greenland based on aerial photographs from 1978–1987. *Sci. Data* **3**, 160032 (2016).
30. van Angelen, J. H., van den Broeke, M. R. & van de Berg, W. J. Momentum budget of the atmospheric boundary layer over the Greenland ice sheet and its surrounding seas. *J. Geophys. Res.* **116**, D10101 (2011).